Reusable glucose fiber sensor for measuring glucose concentration in serum

Cheng-Chih Hsu (許正治)[1*], Yi-Cheng Chen (陳奕誠)[1], Ju-Yi Lee (李朱育)[2], and Chyan-Chyi Wu (吳乾琦)[3]

[1]*Department of Photonics Engineering, Yuan Ze University, 135, Yuan-Tung Road, Chung-Li 32003, China*

[2]*Institute of Opto-Mechatronics Engineering, National Central University, 300, Jhongda Road, Chung-Li 32001, China*

[3]*Department of Mechanical and Electro-Mechanical Engineering, Tamkang University,*

151, Yingzhuan Road, Tamsui 25137, China

*Corresponding author: cchsu@saturn.yzu.edu.tw

We demonstrate a glucose fiber sensor for measuring glucose concentration in serum. High resolution and rapid measurement are achieved through the integration of highly selective enzymes and heterodyne interferometry. The best resolution and response time obtained are 0.14 mg/dL and 1.3 s, respectively. The stability of the sensor is also verified by investigating the initial phase variation. Experimental results show that the fiber sensor can be reused more than 10 times.

OCIS codes: 060.2370, 060.2840, 120.3180, 120.5050.

doi: 10.3788/COL201109.100608.

Fiber sensors have attracted considerable attention over the past two decades. Various kinds of fiber sensors have been proposed for measuring specific chemical concentrations[1−8]. Most previously reported methods[1−5] involved measuring the variations in fluorescence intensity[2−4] or transmitted light[3,4]. Hence, avoiding the influence of surrounding light and the use of expensive photon detection equipment are important requirements. Furthermore, procedures for manufacturing optical biosensors are complicated[3] and quality is difficult to control[4]. The method in Ref. [1] involved the use of the phase delay method in measuring fluorescence lifetime with light emitting diode (LED) intensity modulation and signal analysis by the lock-in technique. This approach may prevent fluctuations in surrounding light and enable the use of economical measurement apparatuses. By contrast, with the phase-measuring technique[6−8], the influence of light intensity can be disregarded so that a photomultiplier is no longer required. However, the sensitivity of this method[6,7] (surface plasmon resonance (SPR) sensor) is strongly influenced by the quality (thickness, roughness, and uniformity) of the deposited metal. Furthermore, the SPR sensor cannot measure a sample with complex compositions unless modified with a specific enzyme. In this letter, we propose a fiber-type measurement system that combines a fiber sensor with heterodyne interferometry to achieve rapid measurement of glucose concentration. The glucose fiber sensor comprises glucose oxidase (GO_x) immobilized on the fiber core by 3-aminopropyltriethoxysilane (APTES) functionalization. GO_x can react only with the glucose to be converted into gluconic acid and hydrogen peroxide, thereby enabling the fabrication of the reusable fiber sensor. Compared with the immobilization method used in Ref. [8], the fiber sensor proposed in the present work exhibits enhanced reusability of up to more than 10 times. As heterodyne light passes through the sensor, the light phase varies as the chemical reaction proceeds, and can be measured immediately by heterodyne interferometry

using the phase-lock technique.

In practice, heterodyne light can comprise linearly polarized He-Ne laser with frequency stabilization control, and an electro-optic modulator (EOM) with the fast axis located at 45° to the x-axis. An external sawtooth voltage signal is applied with an angular frequency and the half-wave voltage $V_{\lambda/2}$ of the EOM is driven by a function generator (Fig. 1). Thus, we have a heterodyne light source with its Jones vector expressed as

$$\mathbf{E} = \mathrm{EOM}(\omega t) \cdot \mathbf{E}_{\mathrm{in}}$$
$$= \begin{pmatrix} e^{i\omega t/2} & 0 \\ 0 & e^{-i\omega t/2} \end{pmatrix} \begin{pmatrix} 1 \\ 1 \end{pmatrix} = \begin{pmatrix} e^{i\omega t/2} \\ e^{-i\omega t/2} \end{pmatrix}. \quad (1)$$

The heterodyne light source is coupled into a single-mode fiber (SMF) with a core diameter of 8 μm using a collimating lens CL_1 with a numerical aperture (NA) of 0.5. The sensing part is a piece of the SMF from which the cladding has been removed, as in the enlarged inset in Fig. 1.

The surface of the core of the glucose fiber sensor was modified by treatment with 5% (v/v) APTES in
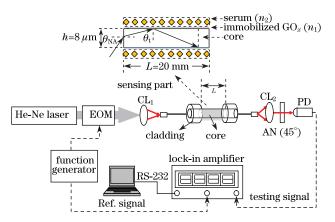

Fig. 1. Schematic of the measurement system and enlarged diagram of the fiber glucose sensor.

ethanol for 10 min at room temperature and heating at 120 °C for 30 min. Then, the surface was covered with 0.005% suberic acid bis (3-sulfo-N-hydroxysuccinimide ester) sodium salt in 10-mmol/L phosphate buffered saline (PBS) for 20 min at room temperature. This procedure was implemented to immobilize GO_x. The modified fibers were immersed into the GO_x solutions with two different pH values (7.5 and 6) of fixed concentrations at 10 μg/mL for 1 h. Then, the unreacted aldehyde groups were quenched by immersion in a 15-mmol/L Tris buffer solution for 10 min at room temperature[9]. As heterodyne light enters the sensing part, the light beam undergoes total internal reflection (TIR). On the basis of the Jones calculation and Fresnel equation[10], the phase difference between the p- and s-polarizations can be expressed as

$$\phi_t = m\phi_{TIR} = \frac{L}{h\tan\theta_t} \cdot \tan^{-1}\left(\frac{\sqrt{\sin^2\theta_t - \left(\frac{n_2}{n_1}\right)^2}}{\tan\theta_t \cdot \sin\theta_t}\right),$$ (2)

where n_1 and n_2 are the refractive indices of GO_x and the testing solution, respectively; θ_t and m are the incident angle and number of TIRs that occur at the interface between GO_x and the testing solution; L (20 mm) and h (8 μm) denote the length of the sensing part and diameter of the fiber core, respectively. After passing through the sensing part, the light beam is collimated by CL_2 (NA = 0.5) and guided through analyzer AN, and then detected by photodetector (PD). The test signal detected by PD can be written as[7]

$$I_t = I_0[1 + \cos(\omega t + \phi_t)].$$ (3)

Reference signal I_r comes from the function generator and can be written as $I_r = I_0'[1 + \cos(\omega t + \phi_r)]$. After sending these two signals into the lock-in amplifier (SR 850, Stanford Research System), the phase difference between the tested and reference signals can be obtained thus:

$$\phi = \phi_t - \phi_r = f(n_1), \quad \text{(before dripping)},$$ (4a)

$$\phi' = \phi_t' - \phi_r = f(n_1, n_2). \quad \text{(after dripping)}.$$ (4b)

Before the testing solution is dripped onto the sensing part, we consider that phase difference ϕ is the function of n_1 and can be regarded as the initial phase difference. Therefore, the activity and stability of GO_x immobilized on the sensor can be determined by examining the initial phase variation. As the testing solution drips onto the sensor, the phase difference varies as the glucose reacts with GO_x to be converted into gluconic acid and hydrogen peroxide; this conversion indicates that refractive index n_2 changes as the chemical reaction proceeds. Hence, phase difference ϕ' is the function of n_2. By comparing phase differences ϕ and ϕ', the absolute phase difference stemming from the chemical reaction can be written as $\Phi = \phi' - \phi = \phi_t' - \phi_t$.

To demonstrate the proposed method, we measured the glucose concentration in human serum. The serum-based sample (SRM 965a) was purchased from the National Institute of Standards and Technology (NIST) and

consisted of eight flame-sealed ampoules of frozen human serum and two ampoules each of four different glucose concentration levels. The four different glucose concentration levels were 34.56, 78.5, 122.1, and 292.6 mg/dL, as certified by NIST following the standard procedure. The pH values of each level were equal to 7.5; 10 μL in volume of each sample was dripped onto the sensor with a pipette (Gilson, Inc.). The fiber sensor was cleaned with the PBS after testing, and then stored in the refrigerator at 4 °C.

Figure 2 shows that the stability of the sensor, determined by studying the variations in initial phase differences ϕ with the number of applications of the sensor. The initial phase difference decreases as the number of applications increases. These results can be contrasted with the chromogen results in Ref. [11] shown in the inset of Fig. 2 (marked A and C). Combining the chromogen and initial phase variation results shows that the sensor becomes inactive when the number of applications exceeds 20. Furthermore, the activity of GO_x on the sensor strongly affects response efficiency and response time. The response efficiency and response time improve with better GO_x activity. On the basis of the results, we conclude that the fiber sensor can be reused about 13 times in one week; this frequency ensures the validity of measurement.

The response efficiency, response time, and slope of the calibration curve are influenced by the pH values of the fiber sensor. Figure 3(a) shows the response efficiency of the sensor given two different pH values when measuring 10 μL in volume of the serum-based sample (level 2 of SRM 965a). The slope of the measurement curve indicates the response efficiency; the sharper the slope, the higher the response efficiency. The response efficiency is higher at pH 7.5 than that at pH 6. In addition, the response time is more rapid at pH 7.5 than that at pH 6, marked A (1.3 s) and B (1.7 s), respectively. Figure 3(b) shows the response time of the sensors at two different pH values of GO_x on the sensor as the level of SRM 965a is measured. Each value shown here is the average of 10 measurement results, and the variation is one standard deviation. According to our results, the shortest response time is about 1.3 s at pH 7.5, with identical sensor and testing sample pH values. The response time is closely related to the similarity in pH between the sensor and testing sample.
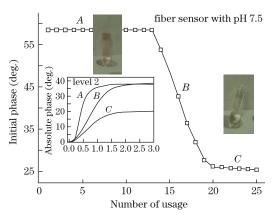

Fig. 2. Initial phase versus number of applications of the sensor, and response curve of the sensor for the corresponding activity state of GO_x.

Figure 4 shows the calibration curves of SRM 965a measured by the sensor with two different pH values. The slopes of the calibration curves are summarized in Table 1. An obvious but small difference in the slopes of the calibration curves is observed between pH 7.5 and 6. The dynamic range of 34–292 mg/dL for the interaction between glucose in serum and GO_x on the sensor is obtained. Resolution Δc of the proposed method can be obtained by calculating the ratio of phase error $|\Delta \Phi|$ to slope s of the calibration curve, represented by $\Delta c = |\Delta \Phi|/s$. Phase error $|\Delta \Phi|$ may stem from the angular resolution of the lock-in amplifier, second harmonic error, polarization-mixing error, and incident angle error because of the misalignment between the collimator and fiber. According to the analytical method discussed in Ref. [8], the phase error can equal $0.02°$. The results shown in Fig. 4 illustrate that the resolution of the
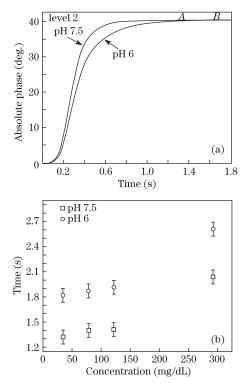

Fig. 3. pH dependence of the response time of the fiber sensor: (a) response curve of the sample (level 2 of SRM 965a) measured at two different pH values of the fiber sensor; (b) response time of all the levels of SRM 965a.
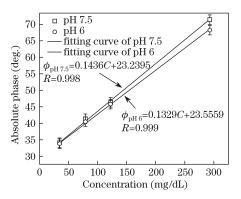

Fig. 4. Calibration curve of the sample with two different sensors (pH 7.5 and 6).

Table 1. Resolution of the Fiber Sensor for SRM 965a

Sensor pH	Sample pH	Slope of Calibration Curve	Resolution (mg/dL)
7.5	7.5	0.1436	0.139
6		0.1329	0.150

proposed method can be determined and is presented in Table 1. The resolution is slightly influenced by the pH properties of the fiber sensor.

In conclusion, we successfully fabricate a glucose fiber sensor with GO_x immobilized on the core surface by APTES functionalization, integrated with heterodyne interferometry. Given the selectivity of GO_x and true phase measurement, the best resolutions are 0.139 and 0.150 mg/dL for measuring the glucose concentration contained in human serum with two different pH values of the fiber sensor. Furthermore, the response times are shorter than 2.2 s for the samples measured by the sensor with pH 7.5. The results show that the pH property of GO_x highly affects response time and response efficiency, but only slightly influences the resolution of the sensor. Therefore, we conclude that identical pH values in the fiber sensor and testing sample enables rapid measurement. In addition, by examining the initial phase variation, we can determine the activity or inactivity of the sensor. The fiber sensor can be reused about 13 times with identical measurement quality.

References

1. D. Jiang, E. Liu, X. Chen, and J. Huang, Chin. Opt. Lett. **1,** 108 (2003).
2. Z. Rosenzweig and R. Kopelman, Sensor. Actuator. B Chem. **36,** 475 (1996).
3. M. Portaccio, M. Lepore, B. D. Ventura, O. Stoilova, N. Manolova, I. Rashkov, and D. G. Mita, J. Sol-Gel Sci. Technol. **50,** 437 (2009).
4. E. Fujii, K. Nakamura, S. Sasaki, D. Citterio, K. Kurihara, and K. Suzzuki, Instrum. Sci. Technol. **31,** 343 (2003).
5. D. S. Bagal, A. Vijayan, R. C. Aiyer, R. N. Karekar, and M. S. Karve, Biosens. Bioelectron. **22,** 3072 (2007).
6. M. Chiu, S. Wand, and R. Chang, Opt. Lett. **30,** 233 (2005).
7. M. Chiu, S. Hsu, and H. Yang, Sensor. Actuator. B Chem. **101,** 322 (2004).
8. T. Lin, Y. Lu, and C. Hsu, Opt. Express **26,** 27560 (2010).
9. A. Peramo, A. Albritton, and G. Matthews, Langmuir **22,** 3228 (2006).
10. P. Yeh, *Optical Waves in Layered Media* (John Wiley & Sons, New York, 1991).
11. D. Barham and P. Trinder, Analyst. **97,** 142 (1972).